Visual Neuroscience (2005), **22**, 345–358. Printed in the USA.
Copyright © 2005 Cambridge University Press 0952-5238/05 $16.00
DOI: 10.1017/S095252380522309X

Sign-conserving amacrine neurons in the fly's external plexiform layer

JOHN K. DOUGLASS AND NICHOLAS J. STRAUSFELD
Arizona Research Laboratories, Division of Neurobiology, University of Arizona, Tucson

(RECEIVED February 3, 2004; ACCEPTED February 16, 2005)

Abstract

Amacrine cells in the external plexiform layer of the fly's lamina have been intracellulary recorded and dye-filled for the first time. The recordings demonstrate that like the lamina's short photoreceptors R1–R6, type 1 lamina amacrine neurons exhibit nonspiking, "sign-conserving" sustained depolarizations in response to illumination. This contrasts with the sign-inverting responses that typify first-order retinotopic relay neurons: monopolar cells L1–L5 and the T1 efferent neuron. The contrast frequency tuning of amacrine neurons is similar to that of photoreceptors and large lamina monopolar cells. Initial observations indicate that lamina amacrine receptive fields are also photoreceptor-like, suggesting either that their inputs originate from a small number of neighboring visual sampling units (VSUs), or that locally generated potentials decay rapidly with displacement. Lamina amacrines also respond to motion, and in one recording these responses were selective for the orientation of moving edges. This functional organization corresponds to the anatomy of amacrine cells, in which postsynaptic inputs from several neighboring photoreceptor endings are linked by a network of very thin distal processes. In this way, each VSU can receive convergent inputs from a surround of amacrine processes. This arrangement is well suited for relaying responses to local intensity fluctuations from neighboring VSUs to a central VSU where amacrines are known to be presynaptic to the dendrites of the T1 efferent. The T1 terminal converges at a deeper level with that of the L2 monopolar cell relaying from the same optic cartridge. Thus, the localized spatial responses and receptor-like temporal response properties of amacrines are consistent with possible roles in lateral inhibition, motion processing, or orientation processing.

Keywords: Early visual processing, Elementary motion detection, Receptive fields, Photoreceptors, Diptera

Introduction

In the fly visual system, as in those of other insects and crustaceans (Strausfeld & Nässel, 1980), the most peripheral amacrine cells originate from cell bodies beneath the lamina, the first level of photoreceptor outputs. Each amacrine cell body sends a stout neurite distally through the lamina's external plexiform layer as far as the surface of this synaptic neuropil, where the neurite divides to provide numerous tangential processes that extend some distance across the lamina. These process provide two types of specializations: swellings at the plexiform layer's surface and varicose specializations, called α processes (Boschek, 1971) that extend down through the plexiform layer. Each α process abuts, and is postsynaptic to, the outer surface of a photoreceptor ending (Campos-Ortega & Strausfeld, 1973).

Receptor terminals in the lamina are arranged in groups of six, each group forming a hollow column (Braitenberg, 1967). Each sextet derives from six rhabdomeres distributed in the retina among six ommatidia. These rhabdomeres sample the same region of visual space and are referred to as a visual sampling unit (VSU; Franceschini, 1975). Each column—also called an optic cartridge—is associated with at least six α processes. These are linked by their tangential fibers to other α processes that reside in neighboring or more distant optic cartridges. Each optic cartridge is equipped with six distinctive types of efferent neurons (Strausfeld, 1970). Three of these, called the large monopolar cells (LMCs) L1, L2, and L3, are postsynaptic to all six receptor endings of their cartridge and thus sample one VSU. However, a fourth efferent neuron, called the T1 basket cell, is not only postsynaptic to all six receptor endings but is also postsynaptic to all the α processes at its optic cartridge (Campos-Ortega & Strausfeld, 1973). Thus, because amacrine processes are linked directly or indirectly to other amacrines at surrounding optic cartridges, each T1 dendritic tree could receive inputs from a surround of nearby optic cartridges. Amacrine neurons thus occupy a unique anatomical position, which is in some respects analogous to that of horizontal cells in the mammalian outer plexiform layer but, as has been proposed from immunocytological studies (Sinakevitch & Strausfeld, 2004), might be functionally comparable to certain types of amacrine cells of the mammalian inner plexiform layer, at the level of bipolar endings.

Address correspondence and reprint requests to: John K. Douglass, Arizona Research Laboratories, Division of Neurobiology, 611 Gould-Simpson Building, University of Arizona, Tucson, AZ 85721, USA. E-mail: jkd@neurobio.arizona.edu

Because they occupy a peripheral location in visual pathways and because their synaptic connections provide a system of lateral connections, lamina amacrines are expected to play a fundamental role in visual processing (Strausfeld & Campos-Ortega, 1977; Shaw, 1984; Douglass & Strausfeld, 2003*a*). For example, they could support wide-field neural adaptation to ambient lighting conditions, lateral inhibition, or, as computational and anatomical models of the lamina suggest, motion detection (Higgins et al., 2004; Douglass & Strausfeld, 2003*a*; Sinakevitch & Strausfeld, 2004). Here, we describe the first intracellular recordings to be clearly identified with lamina amacrines. These recordings reveal response properties that are consistent with a spatially localized role in lateral inhibition and/or motion computation.

Materials and methods

Flies used for intracellular recordings (*Phaenicia sericata*) were raised and maintained in the laboratory under a 12-h light/12-h dark cycle at 25°C, as described previously (Douglass & Strausfeld, 1998, 2003*b*). Ultrastructural and Golgi observations derive from *P. sericata* and *Musca domestica*, also reared under these conditions. We find no difference between the anatomical features of the lamina in these two species. The methods of intracellular recording, computerized visual stimulus presentation, and histological processing were similar to those described previously (Douglass & Strausfeld, 1996, 1998, 2003*b*), with new features as described below.

Electrophysiology

Flies were immobilized with a low-melting point mixture of beeswax and violin rosin and fixed to a pedestal in front of a 300 × 218 mm computer-controlled CRT display that was used to present visual stimuli. Room temperature was approximately 20°C. The fly's eyes were positioned 18 cm from the center of the display, or in some cases the distance was set at 12.5 cm to provide brighter stimuli. Thus, at the fly's head, the stimulus display was "full-field" at either 80 deg wide × 62 deg high (at 18 cm), or 100 deg wide × 82 deg high (at 12.5 cm). The fly and pedestal were attached to a vibration isolation table (TMC 78 Series, Peabody, MA) under a Faraday cage, with the fly's head aligned either for a binocular frontal view, or rotated approximately 45 deg for a lateral, monocular view of the monitor. The fly viewed the monitor through a rectangular opening cut in one side of the Faraday cage, and the opening was covered with a grounded indium-titanium oxide-coated glass plate (Thin Film Devices, Anaheim, CA) to shield the preparation from high-frequency CRT noise. The fly's thorax and abdomen were fixed at 45 deg from horizontal, bringing the head of the fly to a horizontal position. The cuticle at the back of the head was removed along with the first few rows of the most dorsal ommatidia of one or the other eye, providing a clear view of the lamina and first optic chiasma. Exposed portions of the brain were flooded with insect saline (after O'Shea & Adams, 1981; buffered with 5.0 mM TES (Sigma, St. Louis, MO) and adjusted to pH 7.2), and air sacs located dorsally and posterior to the brain were carefully removed using forceps and cactus spines.

Single neurons were impaled in the right lamina or the outer chiasma, using sharp borosilicate or quartz pipettes that were fabricated with a laser puller (P2000, Sutter Instruments, Novato, CA) and backfilled either with 4% Lucifer yellow CH (lithium salt, Molecular Probes, Eugene, OR) and 0.1–0.2M LiCl, or with 10% Neurobiotin (Vector Laboratories, Burlingame, CA) and 1 M KCl. The pipette was connected to the headstage of an intracellular amplifier (Axoprobe 1A, Axon Instruments, Foster City, CA) *via* a chlorided silver electrode, and a silver wire immersed in insect saline behind the brain served as the ground electrode. *In situ* pipette resistances were from *ca.* 120–260 MΩ. The headstage was attached to a micromanipulator (Leica, Bannockburn, IL), the manual fine advance of which was augmented by a piezoelectric drive (IW-800, Burleigh Instruments, Fishers, NY) that was configured to advance the pipette in rapid, 0.5-μm steps. The amplifier "buzz" and the piezoelectric drive were used to assist in penetrations. Recordings showed initial membrane potentials from *ca.* −50 mV to −30 mV, and were continued from 2–20 min prior to iontophoretic injection of Lucifer yellow (−1 to 3nA) or Neurobiotin (+1 to 3nA), using constant current or 1-Hz current pulses.

Intracellular voltages were amplified and digitized at 20 kHz for storage on a PC hard disk (Power 1401 with Spike 2 version 5 software, Cambridge Electronic Design (CED), Cambridge, England). Additional analog/digital (A/D) channels recorded a voice record of events during each experiment, as well as stimulus timing signals provided by two photodiodes (PIN 10 DP, United Detector Technologies, Hawthorne, CA) that received, respectively, small-field and wide-field views of the CRT display (Douglass & Strausfeld, 2003*b*).

Visual stimuli

During intracellular recordings, visual stimuli were presented using Visionworks Neurosequence v3.0 software, a VGA adapter, and a custom monochrome monitor equipped with ultrashort persistence green "P46" phosphors and operated at a vertical refresh rate of 200 Hz (Vision Research Graphics, Durham, NH). Stimulus irradiance spectra and absolute irradiances at the position of the fly's head (integrated from 300–700 nm) were measured with a fixed-grating spectrometer (model S2000 with "Ooirrad2" software, Ocean Optics, Dunedin, FL), fitted with a 100-μm-diameter fiber optic cable designed to transmit ultraviolet (UV) and visible wavelengths. The input end of the fiber optic was fitted with a cosine collector, and the spectrometer was operated with sufficiently long integration times to encompass multiple vertical retraces of the stimulus monitor. The spectrometer is calibrated in this configuration to an NIST-traceable standard tungsten lamp (Ocean Optics LS-1-CAL). The monitor's irradiance spectrum shows a single broad peak region from 510–590 nm, with a full half-bandwidth of 110 nm. With the display set for maximum brightness, the absolute irradiance of a 10-mm-diameter circle measured at a distance of 125 mm from the CRT was approximately 4×10^{10} $q \cdot cm^{-2} \cdot s^{-1}$.

Visual stimuli included full-field square-wave flicker, full-field square-wave grating motion, and horizontal or vertical motion of single bright bars. All stimuli were defined with constant pixel dimensions, and (if applicable) a constant onscreen speed and the maximum possible brightness per pixel. Thus, for a given neuron, the *apparent* dimensions and speeds of stimuli were partly a function of the viewing distance and the location of the receptive field. Except where noted in the Results for bar motion stimulation, these considerations do not affect the conclusions regarding the basic response properties of lamina amacrines.

The full-field flicker stimulus was designed to test basic On/Off responses as well as temporal response properties, and was comprised of a series of logarithmically spaced flicker frequencies ranging from 1 Hz to 100 Hz and back to 1 Hz. The grating motion was presented in eight directions to test for sensitivity to motion

orientation or direction, at speeds and spatial frequencies that are known to produce robust responses in lamina neurons and elsewhere in the dipteran visual system (e.g. Laughlin, 1981; Hengstenberg, 1982; Douglass & Strausfeld, 1996). Each single vertical or horizontal bar extended the full height or width of the CRT display, and was moved from one edge of the display to the other (from left-to-right or top-to-bottom) and back again. Single bar motion provides a rapid means of evaluating the location and spatial extent of a cell's receptive field, while simultaneously testing for sensitivity to the direction of edge motion. Spatial receptive-field properties were also evaluated by presenting brief flashes of stationary circles, which appeared one at a time in a pseudorandom sequence of 48 overlapping locations such that no two successive positions were adjacent (see Fig. 4A).

Histology and anatomical reconstructions

Following intracellular recording and staining, the brain was removed from the head capsule, fixed in phosphate-buffered 4% formaldehyde, and rinsed in Millonig's phosphate buffered saline (PBS). For neurobiotin-stained preparations, the brain was permeabilized by dehydration in an alcohol series to propylene oxide, rehydration, treatment with 0.1% Triton-X-PBS, and incubation in 1:5000 avidin-Texas Red conjugate (Molecular Probes) in PBS. All brains were then dehydrated again, embedded in Spurr's plastic, sectioned on a sliding microtome, and viewed with a confocal epifluorescence microscope (LSM 5 Pascal, Carl Zeiss, Thornwood, NY). Fluorescent profiles of intracellularly stained neurons were identified according to characteristic morphological features that are well known from previous anatomical studies of the dipteran optic lobe (Strausfeld, 1976, 1989; Strausfeld & Nässel, 1980).

Golgi impregnations

Opened heads were processed using a previously described combined Golgi Colonnier-Golgi rapid method (Strausfeld & Li, 1999). Observations on lamina amacrines take into account impregnated cells at locations that include the frontal, lateral, ventral, and dorsal fields of view.

Electron microscopy

The compound eye was sliced open and then it and its optic lobe, as far as the level of the medulla, were removed from the head under fixative comprising 2.5% EM grade glutaraldehyde and 2% EM grade formaldehyde (Electron Microscopy Sciences, Ft. Washington, PA) carried in 0.1 M Millonig's PBS, pH. 7.2. After 12 h fixation at room temperature, tissue was washed in buffer, immersed in 0.1% osmium tetroxide (in water) for 12 h at room temperature, then washed, dehydrated, and embedded in Durcupan plastic *via* propylene oxide. Ten-micron sections were cut on a sliding microtome, mounted between gelatin sheets in Durcupan, and examined under a compound microscope. Those parallel to the outer surface of the plexiform layer were removed, reembedded, polymerized, and then serial-sectioned with a Reichardt ultramicrotome to obtain silver to gray sections. Sections were mounted on copper grids, stained with lead citrate and uranyl acetate, and examined with a JEOL 2000 electron microscope. Negatives were digitally scanned, then converted to positive images using Adobe Photoshop.

Data analysis

Electrophysiological data were analyzed with Spike 2 (version 5, CED), Excel 2000 (Microsoft) and Origin 7.5 (OriginLab, Northampton, MA). Raw intracellular records were low-pass filtered (Spike 2 finite impulse response filter) above 100 Hz to attenuate high-frequency noise (-3 dB point = 167 Hz). Data analysis scripts written in Spike2 were used to measure response parameters from voltage traces by using manually placed markers. Flicker response amplitudes and latencies were measured from the prestimulus "On" or "Off" baseline membrane voltage to the maximum response level. The latency was defined as the intersection of the prestimulus baseline with a line defined by the points where the intracellular voltage reached 20% and 80% of the maximum initial upward or downward deflection. Stimulus On and Off times were obtained from the photodiode record of each vertical CRT scan within a small circular region at the center of the stimulus monitor. The flicker latency measurements therefore incorporate a $\pm$ 2.5 ms correction according to the vertical distance of a cell's receptive field from the center of the display.

Results

Amacrine morphology

Salient anatomical features of lamina amacrine cells are illustrated in Fig. 1. The large, ellipsoid-shaped cell bodies of type 1 lamina amacrines (Fig. 1G) lie 10–20 μm proximal to the lamina among axons forming the outer part of the first optic chiasma, and are the only neurons originating from this level. Cell bodies of lamina monopolar cells lie distal to the plexiform layer. The cell bodies of T1 efferent neurons, as well as those of centrifugal tangential cells, lie above the medulla and are displaced to the side of the inner part of the first optic chiasma (Strausfeld, 1976).

The arborizations of type 1 lamina amacrines are distinctive, reflecting the known synaptic relationships of their α processes with photoreceptor terminals and T1 efferent neurons (Campos-Ortega & Strausfeld, 1973). The plexus of tangential processes that extends over the outer surface of the plexiform layer is less well described. Where the tangential processes of several amacrines converge and intermingle, above and to the side of each optic cartridge (Figs. 1A & 1B), they give rise to varicose swellings. Electron microscopy of these tangential processes suggests that amacrines are presynaptic and postsynaptic to each other at these nodes, and can be postsynaptic to receptor endings as well at this distal level (Figs. 1C–1E). The tangential processes provide a system of looped fibers that first extend down through the plexiform layer and then recurve to provide a tuberous specialization, called the α process (Fig. 1F), which ascends up the outside of the cartridge alongside a receptor ending. Each α process gives rise to a comb of spines to one side. Previous electron-microscopical studies of muscid and calliphorid flies (Boschek, 1971; Campos-Ortega & Strausfeld, 1973) have identified these tubers as being postsynaptic to receptor endings, as they also are in *Drosophila* (Meinertzhagen & O'Neil, 1991). Immunocytology reveals type 1 amacrines to be immunoreactive to sera raised against the neurotransmitter, glutamate (Sinakevitch & Strausfeld, 2004). The α processes also have been shown to be presynaptic to the dendrites of T1 efferent neurons (Campos-Ortega & Strausfeld, 1973), the dendrites of which correspond to elements that are revealed by antibodies against a NMDAR1 receptor protein (Sinakevitch & Strausfeld, 2004).

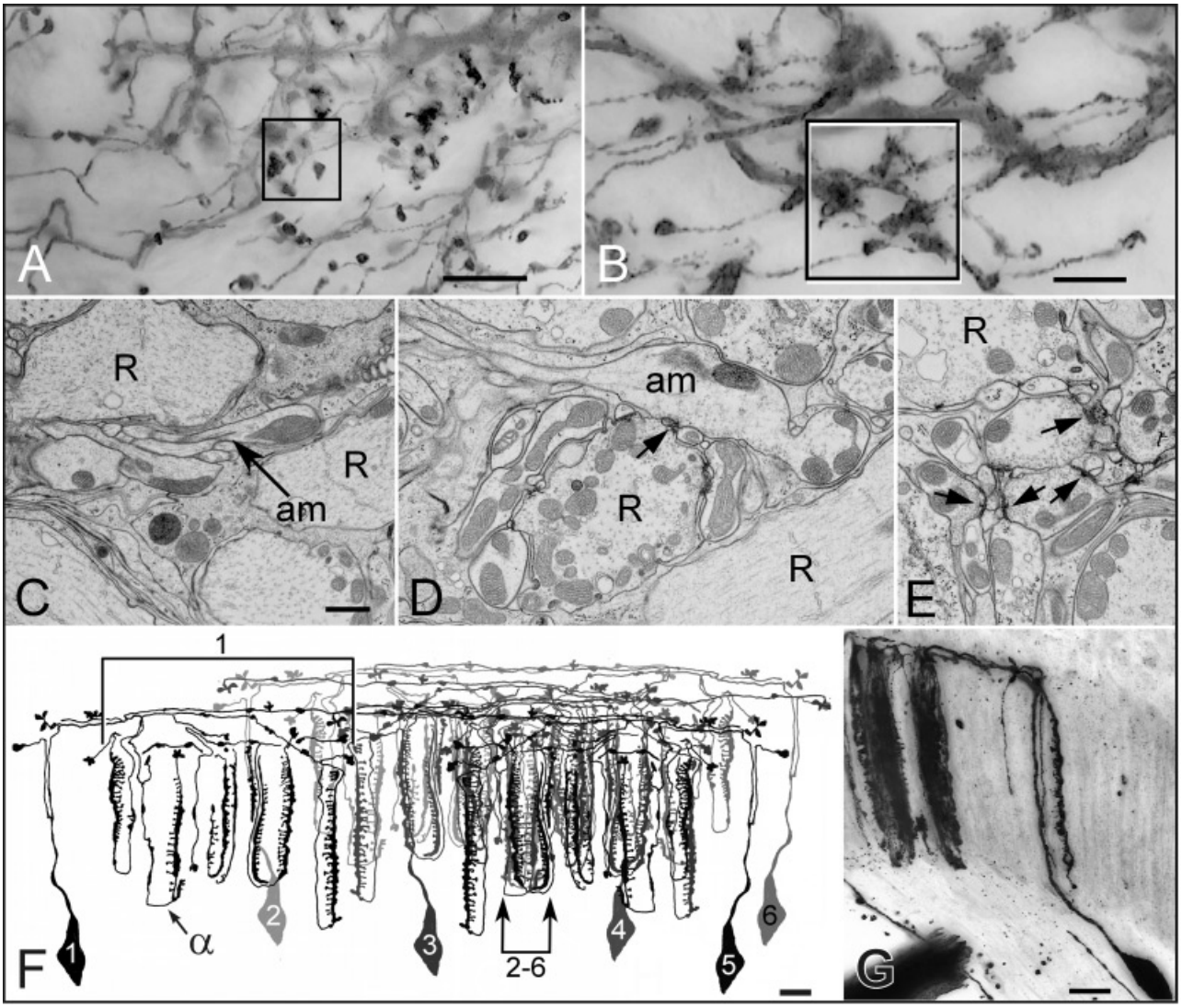

Fig. 1. Anatomical characteristics of lamina amacrine cells, revealed by Golgi staining and electron microscopy. (A) Golgi impregnation showing a top–down view of the superficial plexus of amacrine tangential processes with regularly spaced nodes comprising varicose specializations (one node shown boxed). (B) Golgi impregnation showing converging processes from several amacrines providing apposed varicose specializations at one node (boxed). (C–E) Low-power electron micrographs showing amacrine tangential process (arrowed am in C), amacrine swellings distal in the lamina (am in D), and convergence of amacrine processes, as in boxed areas, denoted by boutons equipped with synaptic specializations (arrowed in D & E). Receptor profiles are labeled R. (F) Lamina amacrines can have various sizes, spreading through between 6 and 12 optic cartridges. In this schematic, the minimal spacing necessary to provide one optic cartridge with its six amacrine processes (indicated by arrowed bracket 2–6) is reconstructed by overlapping five identical amacrine cells (2–6), the shapes of which correspond to the single element (1) shown to the left, which supplies one or two α processes to each of five optic cartridges (under bracket 1). (G) Golgi-impregnated amacrine including cell body and cell body fiber. Scale for A = 10 μm; scale for B = 5 μm; 1 μm scale in C also applies to D, E. Scales for F,G = 10 μm.

Amacrine cells extend across several cartridges. The smallest domain observed was eight cartridges in close proximity, where a single amacrine provided two α processes to three adjacent cartridges and one α process to a fourth cartridge. Other amacrines have been observed with wider spreads. However, each cartridge is equipped with six α processes, and a regular network of tangential amacrine processes covers the surface of the plexiform layer, providing a symmetrical arrangement of synaptic nodes. Thus, despite the individual variation in the size of their domains, amacrines together provide an isotropic organization across the entire lamina. Presynaptic and postsynaptic connections within this plexus allow each α process at one cartridge to be connected to the α processes that supply surrounding cartridges. For example, even amacrines with quite small domains can be diffusely arranged yet still contribute six α processes to several cartridges (Fig. 1F).

As will become clear below, the visual responses of lamina amacrines and photoreceptors are very similar, at least in their basic features. As a result, in preparations that include both amacrine and photoreceptor staining, it can be difficult to identify the source of the recording. To avoid mistaken identification of a recording, the following criteria were used for identifying a lamina amacrine recording: (1) basic responses that are "sign-conserving"

(as in photoreceptors), (2) the absence of any stained photoreceptor that could account for these responses, and (3) a retinotopic location of the stained amacrine material that is consistent with the physiologically determined receptive-field location. Among several type 1 lamina amacrines that have been intracellularly stained to date, three preparations satisfy these criteria. All of the data we attribute to amacrines are derived from these three preparations. Similarly, all data attributed to photoreceptors are from recordings that were clearly identified with one or more stained photoreceptor terminals in the lamina and thus belong to R1–R6 receptors.

Fig. 2 shows examples of intracellularly stained fluorescent profiles belonging to the three type 1 lamina amacrines mentioned above (panels numbered i–iii), as well as a fourth amacrine that was co-stained with several photoreceptors and thus did not satisfy the above criteria (panel iv). The boxed profiles are clearly identifiable as portions of lamina amacrines, as they correspond to the characteristic morphological features that have been boxed in the accompanying drawing of a complete lamina amacrine cell. These features include a superficial plexus that connects varicose specializations (Fig. 2, see boxes labeled "A"), a cell body located beneath the lamina, with the cell body fiber extending to the outer surface of the lamina (Fig. 2 "B" boxes), relatively thick columnar fibers that are located in the spaces between unstained photoreceptor terminals and which may be seen with or without clear evidence of dendritic specializations (Figs. 2C and 2D boxes, respectively), and columnar α loops in the inner lamina (Fig. 2E boxes). In the Lucifer yellow-stained preparation (Fig. 2, panel i), the dye appears to have extended beyond the boundary expected from a Golgi impregnation of a single lamina amacrine cell. Dye migration into the processes of one or more adjacent amacrines is not implausible, as some distal profiles within the amacrine-to-amacrine tangential network appear to possess small gap junction-like zones (N.J. Strausfeld, personal observation), which could permit migration of Lucifer yellow to other amacrines.

Physiological properties of amacrine neurons

We now turn to the physiological recordings from lamina amacrines i–iii, and compare their properties with those of other lamina neurons. Previous intracellular investigations have documented the basic electrophysiological properties of most of the 20 distinguished types of lamina neurons. These include the eight photoreceptor types R1–R8, five lamina monopolar cell types, a type of centrifugal tangential neuron to the lamina known as Lam Tan 1, the small-field centrifugal cell C2, and the T1 neuron (see Discussion for details). Here, we focus on comparing lamina amacrine responses with those of photoreceptors, because these

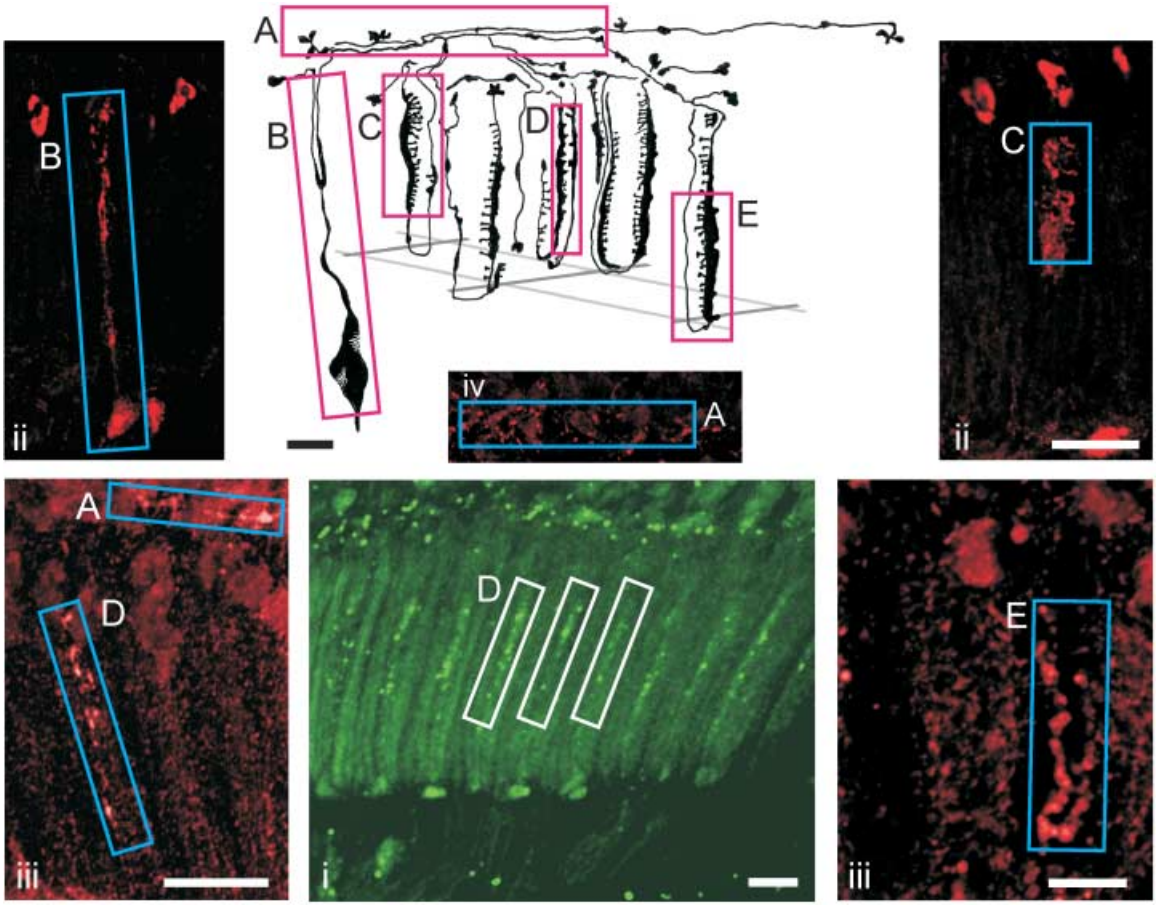

Fig. 2. Characteristic structures of four intracellularly stained lamina amacrine neurons denoted i–iv in the text. Type 1 lamina amacrines are clearly identifiable according to characteristic morphological features (*boxed* in blue and white) that have previously been identified from Golgi-stained material (*red boxes* A–E). All figures are oriented with the outer lamina up and the first optic chiasma down. Scale bar = 20 μm for i, ii, iv, and center diagram; 10 μm for iii.

two types share certain basic properties which distinguish them from all other known lamina neurons.

The photoreceptors of insects (Burkhardt & Autrum, 1960; Washizu et al., 1964; Järvilehto & Zettler, 1973) and other invertebrates are well known to exhibit "sign-conserving" responses with respect to the sign of a change in stimulus intensity: an increase in illumination produces a graded depolarization, whereas a decrease in illumination results in hyperpolarization. The photoreceptors R1–R8 all share this characteristic, although the long visual fibers R7 and R8 differ from R1–R6 in other ways that include their terminations in the medulla, their spectral sensitivities (reviewed by Hardie, 1986), and more subtle aspects that are relevant to their information-processing properties (Anderson & Laughlin, 2000). An example of sign-conserving flicker responses of a type 1–6 receptor (in this case co-stained with 3–4 neighboring R1–R6 receptors, Fig. 3A) is shown in Fig. 3B. Photoreceptor responses to grating motion (Fig. 3C) are phase-locked to the grating contrast frequency, as expected for a relatively small-field neuron responding to the local intensity fluctuations as bright and dark bars pass alternately over the receptive field.

In contrast with photoreceptor responses, monopolar cells and other intracellularly recorded lamina neurons typically exhibit "sign-inverting" responses. The flicker responses of LMCs, such as L2 (Fig. 3D, here co-stained with an L1 and an L3 LMC belonging to the same retinotopic column), are typified by a transient on-hyperpolarization and transient off-depolarization (Fig. 3E). Depending on recording conditions, the on-hyperpolarization of LMCs may also include a sustained component (Järvilehto & Zettler, 1973; Laughlin, 1981). It was not possible to test grating motion responses in this recording, but these have been documented previously in recordings from both large monopolar cells (e.g. Gilbert et al., 1991; L1–L3) and small monopolar cells (Douglass & Strausfeld, 1995; L4 and L5).

Figs. 3F–3K show staining and responses of two lamina amacrines that were first introduced in Fig. 2 (amacrine i, Figs. 3F–3H; amacrine iii, Figs. 3I–3K). Both recordings show sign-conserving flicker responses (Figs. 3G & 3J) and contrast frequency-dependent sinusoidal fluctuations in response to grating motion (Figs. 3H & 3K). The flicker responses of these two cells clearly differ in their details, however, and are chosen to illustrate what may represent

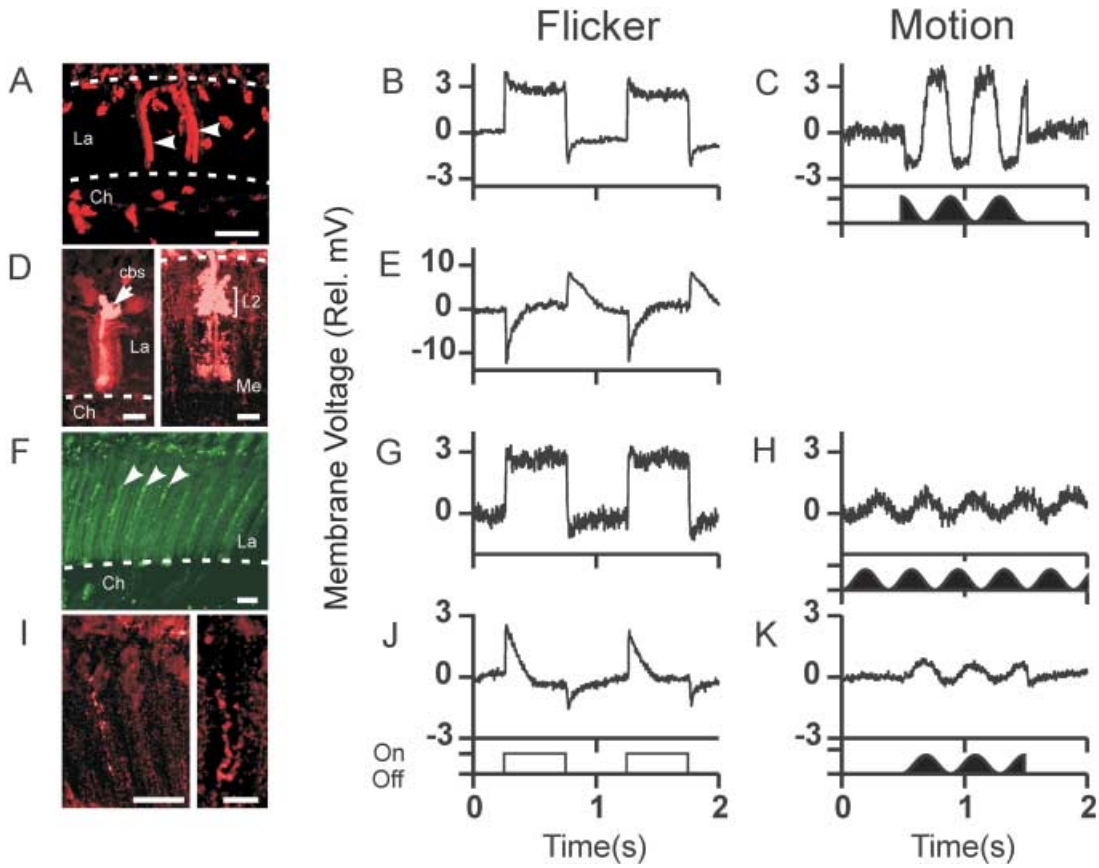

Fig. 3. Intracellular responses of identified lamina neurons to full-field flicker (B, E, G, & J) and horizontal grating motion (C, H, & K). La, lamina; Ch, first optic chiasm; Me, medulla. (A–C) Example of a recording from an R1–R6 type photoreceptor, corresponding to one of the stained receptor terminals in A (arrowheads). Flicker responses (B) are sign conserving, and grating motion responses (C) follow the contrast frequency as indicated below the voltage trace. (D, E) Example of sign-inverting responses, in this case from an L2 neuron that was co-stained with an L1 and L3 belonging to the same retinotopic column (The trace is presumed to correspond to the more brightly stained L2). (F–H) amacrine i, showing staining of α processes in the lamina (F), sign-conserving flicker responses (G), and grating motion responses (H). (I–K) Amacrine iii, showing staining of α processes (I), sign-conserving flicker responses (J) including a small transient Off-hyperpolarization and rapid decay of the On depolarization, and grating motion responses (K). The photoreceptor and amacrine i recordings were obtained with the fly's head positioned at 18 cm from the stimulus monitor, or 12.5 cm for the L2 and amacrine iii. All responses are zeroed to the prestimulus baseline level to facilitate comparisons. Note that the voltage scales span different ranges of 8 mV (B & C), 28 mV (E), and 6 mV (G, H, J, & K).

two extremes in the possible range of lamina amacrine responses to abrupt changes in stimulus intensity. Amacrine i (Fig. 3G) showed a sustained "On" depolarization and little or no "Off" hyperpolarization beyond the baseline. In amacrine iii (Fig. 3J), the On-depolarizations initially lacked a strong sustained component, instead showing a gradual decay toward the baseline voltage level, followed by a transient Off-hyperpolarization. Later in the recording from amacrine iii (data not shown), its depolarizing activity became gradually more "sustained," yet the hyperpolarizing Off transients persisted. In conclusion, the responses of lamina amacrines to wide-field flicker are fundamentally sign-conserving, as in photoreceptors. This basic characteristic has also been confirmed in lamina amacrine ii, which was not stimulated with flicker, but nonetheless exhibited robust sign-conserving responses to single bar motion (see Fig. 5B below).

Figs. 3C, 3H, and 3K compare the responses of the photoreceptor and amacrines i and iii to movement of a wide-field vertical grating. Although these amacrine motion responses are weak compared to the flicker responses, this appears to reflect the fact that grating motion was presented late in these two recordings, when overall response amplitudes were diminishing. Nevertheless, the mere presence of voltage fluctuations at the grating contrast frequency provides an initial clue about the spatial receptive-field properties of lamina amacrines. In general, if the wavelength of a high-contrast grating is far less than the diameter of a neuron's principal receptive field, then grating motions should produce little or no fluctuation in membrane voltage. If the grating wavelength is much greater than the receptive-field diameter, one can expect to see relatively sudden depolarizations and repolarizations, with intervening periods when the voltage remains relatively stable. The present recordings suggest that in these two amacrines, as in the photoreceptor, the approximate limits of the principal receptive-field region were roughly comparable to the grating stripe width (half of the grating wavelength). The apparent stripe width depends on the viewing distance and the receptive-field location on the stimulus screen, which was possible to estimate in some recordings according to the responses to single bar motion (see below). For the receptor in Figs. 3A–3C, the apparent stripe width was approximately 9 deg. For amacrine i, the receptive-field location is unknown, but the grating dimensions at the center of the display predict an upper limit of 10 deg for the apparent stripe width. For amacrine iii (from a fly that was positioned closer to the display), the apparent stripe width was approximately 14 deg. Thus, without embarking upon a more detailed analysis, the grating motion responses in Fig. 3 suggest that lamina amacrines and photoreceptors have very comparable spatial receptive-field properties.

Two additional measures of spatial receptive-field properties are provided by responses to flashing stationary circular spots and to bar motion. Fig. 4A illustrates an 8×6 array of overlapping circles which were presented in a pseudorandom sequence of 48 individual "flicker" flashes (for spot dimensions, see Fig. 4 caption). This stimulus has been used during several recordings from photoreceptors, and despite the large size of the flashed spots compared to full-width half-maximum acceptance angles of less than 2 deg (Burton et al., 2001), it is possible for several of the spots to elicit a photoreceptor response due to their mutual overlap and the more extensive receptive field beyond the region of greatest sensitivity (Smakman et al., 1984). The stationary flash stimulus was also presented during the recording from amacrine iii. The contour plots in Fig. 4 compare its responses (Fig. 4B) with those of two identified photoreceptors (Figs. 4C & 4D). Like the grating motion responses above, these results are suggestive of similar spatial receptive fields in lamina amacrines and photoreceptors. Due to the large size of the flash stimuli, however, these data still only offer a low-resolution glimpse of actual receptive fields. Some experiments have also tested responses to spots as small as 6 deg in diameter (the smallest size that produces a reliable response due to the limited brightness of the CRT display), but to date, none of these recordings has subsequently been identified with an amacrine cell.

The most detailed information to date on the receptive-field properties of amacrines has come from two recordings of responses to single moving bars. The voltage traces in Fig. 5 compare photoreceptor (Fig. 5A), amacrine ii (Fig. 5B), and amacrine iii (Figs. 5C–5E) responses to a sequence of bar motions in four directions; these were interspersed with full-field On and Off flicker stimuli. Ignoring the flicker responses for the moment, three distinct aspects of the bar motion responses reveal crucial features of the recorded neurons' response characteristics. First, the *timing* of the maximal responses to bar motion discloses the approximate horizontal and vertical coordinates of the receptive field. These are illustrated in the insets to Figs. 5A–5C, and indicate that the receptive-field center of the photoreceptor (Fig. 5A) viewed a point approximately 8 deg from the center of the CRT, whereas those of amacrine ii and iii (Figs. 5B–5E) were some 30 deg and 10 deg from the center, respectively.

A second useful aspect of the responses to bar motion is their durations; these provide information concerning the horizontal and vertical extent of the recorded neuron's receptive-field as a function of the width of a moving bar. The apparent width of a bar, however, depends not only on its fixed physical dimensions, but also on the distance from the fly's head to the CRT and the position of each neuron's receptive-field center. Thus, for the two *physical* bar widths used in these experiments, these parameters were used to compute the *apparent* bar widths shown in the upper right corner of each voltage trace. In general, the photoreceptor (A) and amacrine (B–E) response durations were similar, consistent with the above lines of evidence that these two types of lamina neuron share comparable spatial characteristics. Other recordings from photoreceptors (not shown) have also shown similar response durations. A closer look at Fig. 5, however, suggests there may be some interesting differences among the receptive-field properties of these neurons. First, comparing the two amacrine recordings, the durations of responses in amacrine ii (Fig. 5B) were about the same as those of amacrine iii (Figs. 5C–5E), despite the substantially wider apparent bar widths seen by amacrine iii. If the two cells had identical receptive-field properties, one would expect amacrine ii to display the shortest response durations. Second, amacrine ii's responses (Fig. 5B) lasted as long or longer than those of the photoreceptor (Fig. 5A), despite the wider apparent bar width for the photoreceptor. These observations suggest that, on an individual basis, there may be receptive-field differences both among amacrines, and between amacrines and photoreceptors.

A third informative feature of the bar motion responses is their amplitudes as a function of motion direction. Whereas amacrine ii and the two photoreceptors (Figs. 5A and 5B) showed nearly symmetrical responses to the four directions of bar motion, the three repeated traces from amacrine iii consistently showed the largest responses to horizontal motion. These patterns are quantified in Fig. 5F, which represents all of the data in Figs. 5A–5E as well as an additional dataset from a second R1–R6 photoreceptor. The polar plots (Fig. 5F) confirm that the responses of amacrine iii were asymmetrical, with stronger responses to horizontal than to vertical motion. Although the resting potential and overall respon-

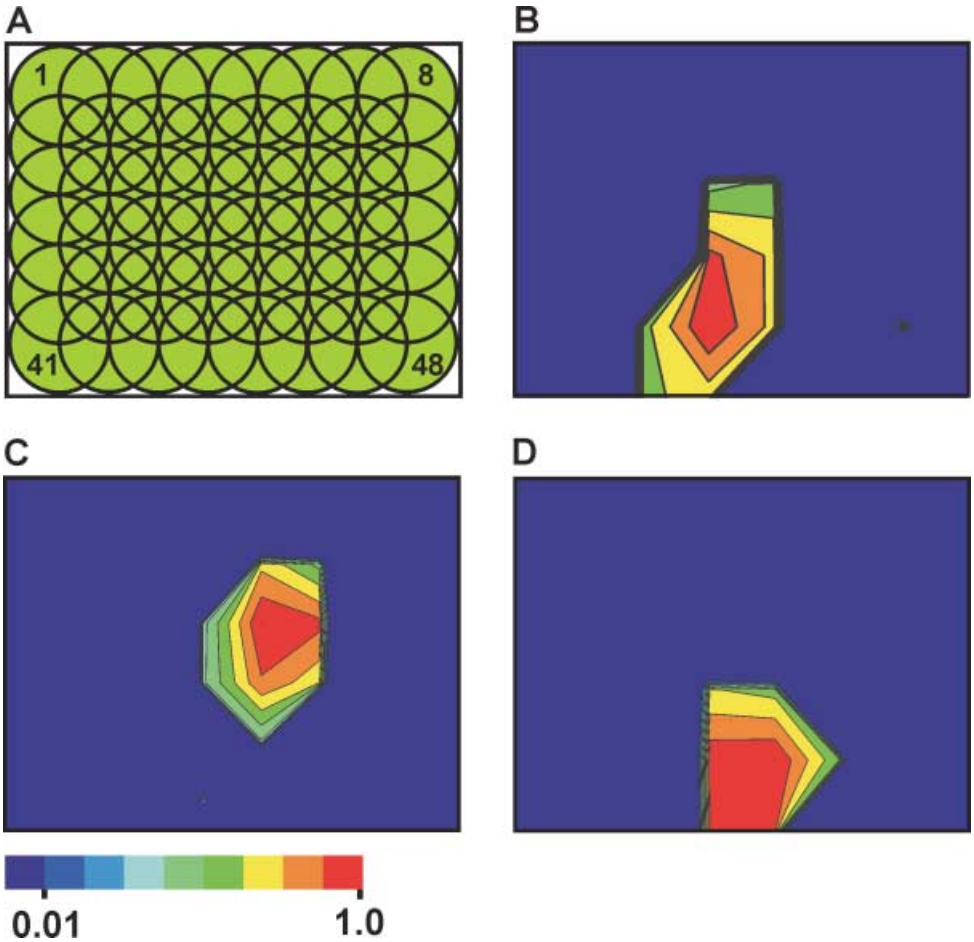

Fig. 4. Spatial receptive-field properties of two photoreceptors and a lamina amacrine, compared by presentation of the stationary flicker stimuli depicted in A. Amplitudes of responses to a randomized sequence of 48 stationary circles (A), each flashed for 120 ms on the 62 × 80 deg stimulus CRT with 50-ms pauses between flashes, were used to construct contour plots (B–D, from normalized log responses), which show the receptive-field location and a representation of its spatial extent. Despite having dendritic fields that can extend across several visual sampling units (VSUs), the spatial response pattern of amacrine iii (B) is roughly similar to those of photoreceptors (C & D). The onscreen diameter of each circle was 57 mm. With the viewing distance of 125 mm for the amacrine (180 mm for the receptors), this corresponds to an angular diameter of 26 deg (or 18 deg for the receptors).

siveness of this neuron gradually diminished during the presentations of bar motion, responses to vertical motion were consistently weaker in all three traces, so this pattern does not merely reflect a deteriorating preparation or gradual adaptation to motion. This conclusion is confirmed by the responses of amacrine iii to grating motion (Fig. 6A), which were obtained later in this recording and show a similar directional asymmetry. In this case, overall response amplitudes remained nearly constant, and the weakest responses (Fig. 6A, *shaded*) were soon followed by stronger responses to other motion directions. Fig. 6B shows the integrated responses as a function of grating motion direction, and demonstrates a strong preferred orientation axis that is consistent with this neuron's bar motion responses (Fig. 5F).

One additional and currently unexplained aspect of the amacrine iii responses deserves mention. During each presentation of bar motion interspersed with wide-field flicker, amacrine iii responded only to the first flicker flash (Figs. 5C–5E), yet the other amacrine (Fig. 5B) and all photoreceptor recordings showed nearly identical responses to these three flashes. Again, the insensitivity of amacrine iii to the second and third flashes does not reflect an overall weakening of this cell's responses, since the motion responses continued both during and after these tests. Given that amacrines also showed no obvious adaptation to a pure wide-field flicker stimulus (see Fig. 7), an intriguing possibility is that a motion-specific inhibitory effect reduced the sensitivity of this amacrine to wide-field flicker.

Contrast frequency sensitivity is another important basic property that is related to the functional roles of visual interneurons. The responses of two photoreceptors and two amacrines across a range of flicker frequencies (examples in Fig. 7A) were used to measure On- and Off-response amplitudes and phase delays as a function of flicker frequency (Fig. 7B). In both groups of recordings, the On-amplitudes and both On- and Off-phase delays were relatively stable from 1 to approximately 30 Hz, falling off more steeply toward higher frequencies. Although the two amacrines showed slightly smaller On-amplitudes and larger phase delays toward higher frequencies, additional recordings would be needed to establish whether these are consistent features of amacrine responses. The only clearly distinctive aspect of the amacrine responses is that for amacrine iii, the Off responses show a peak amplitude between 5 and 40 Hz. This difference simply results from the slowly decaying On response in this particular recording

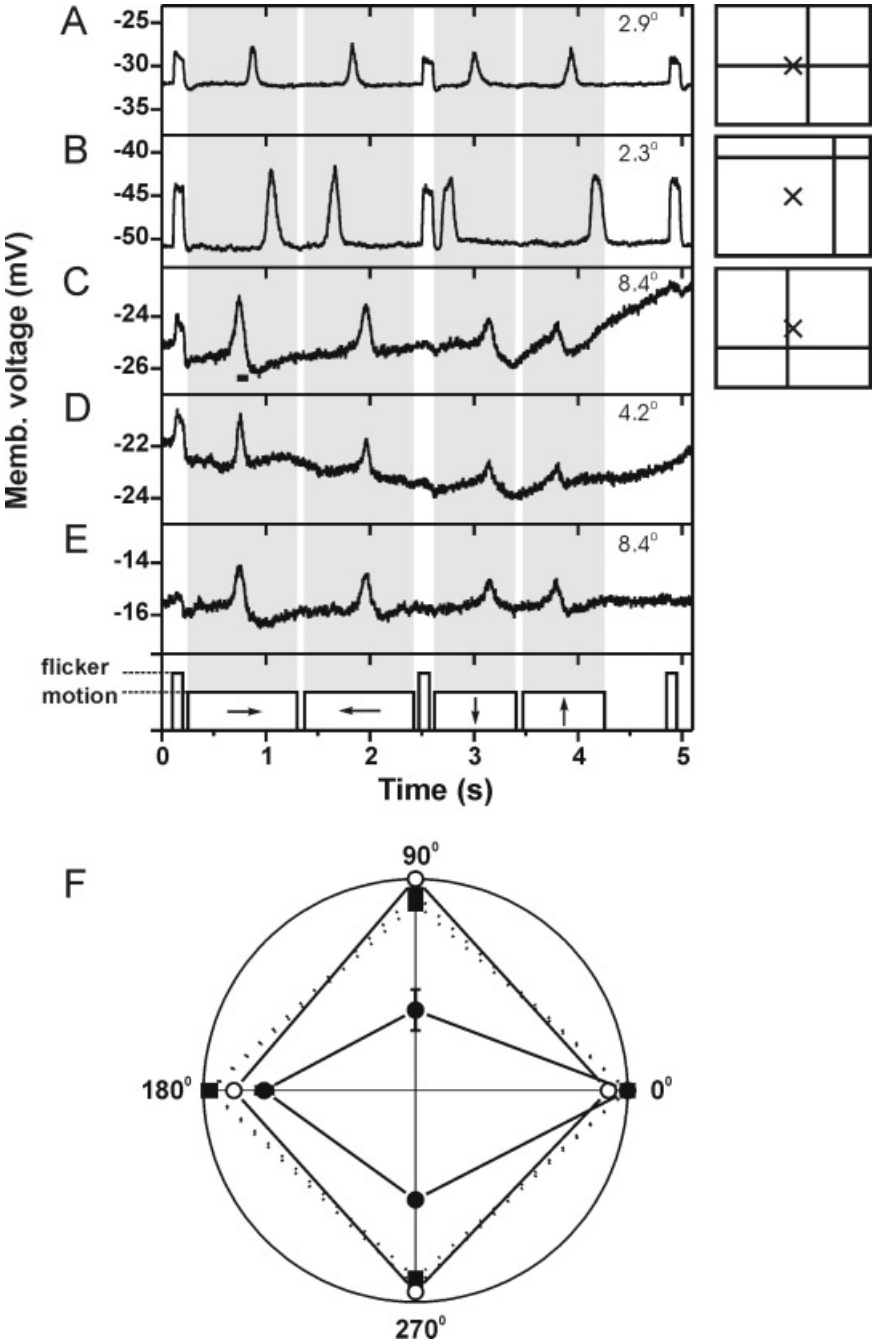

Fig. 5. Spatial receptive-field properties and motion responses of a photoreceptor (A) and lamina amacrines ii (B) and iii (C–E), revealed by responses to motion of single bright bars on a dark background. Each voltage trace shows responses to a sequence of single bar motion in four directions, bracketed with intervening full-field flicker. The first flicker flash (see legend below traces) was followed by rightward then leftward motion of a bright vertical bar (*arrows*), a second flash approximately at $t = 2.5$ s, downward and upward motion of the corresponding horizontal bar, then a final flash. (A) Photoreceptor responses with the fly's eye positioned 18 cm from the stimulus CRT. (B) Amacrine ii responses, also at 18 cm. (C–E) Responses of amacrine cell iii, with the eye positioned at 12.5 cm. The timing of the maximal responses to bar motion reveals the approximate horizontal and vertical coordinates of the receptive field, as illustrated by crosshairs within the rectangular stimulus region (A–C insets; X marks the center of the display). The apparent bar width is indicated in the upper right corner of each trace, based on the receptive-field location, viewing distance, and one of two physical bar widths (3 deg or 6 deg) that were available for presentation. (F) Polar plot showing normalized responses to bar motion (integrated voltages above baseline) as a function of motion direction. Solid lines show the symmetrical responses of amacrine cell ii (—○—, from trace B) and asymmetrical responses of amacrine iii (—●—, N= 3 from traces C–E, mean ± S.E.). The dotted lines connecting square points show symmetrical responses of two photoreceptors (the raw data for one of these appear in A). Response amplitudes were quantified by manually marking the time (t_p) of the response peak, then computing the integrated difference from the baseline voltage during the peak interval from (t_p − 140) ms to (t_p + 140) ms. The baseline voltage was defined as the mean prestimulus and poststimulus baseline, measured from the two 50-ms periods surrounding each peak interval.

(see Fig. 3J), which made the baseline for the Off response highly dependent on the flicker frequency. In conclusion, these lamina amacrine recordings demonstrate robust responses across a broad range of flicker frequencies, and in this respect the temporal response properties of lamina amacrines are closely matched to those of photoreceptors.

Discussion

Identification of lamina amacrine and photoreceptor recordings

This study presents the first physiological recordings to be identified with amacrines in the insect lamina. Based on the specific criteria described in the Results, three intracellular recordings were identified with stained elements of type 1 lamina amacrines, and to the extent that it was possible to present the same stimuli to different preparations, the basic responses in all three recordings are internally consistent. Thus, we are confident that these recordings have been correctly identified. We are aware of one previous, though tentative suggestion, based on a single recording from the fleshfly, *Rutilia* (Ioannides, 1972), that an intracellular trace might correspond to a lamina amacrine. In this case, however, the diffusely stained material that was illustrated did not correspond to the characteristic anatomical features of lamina amacrines which are known in Diptera, and in any case the only voltage trace provided showed no clear response to a flash.

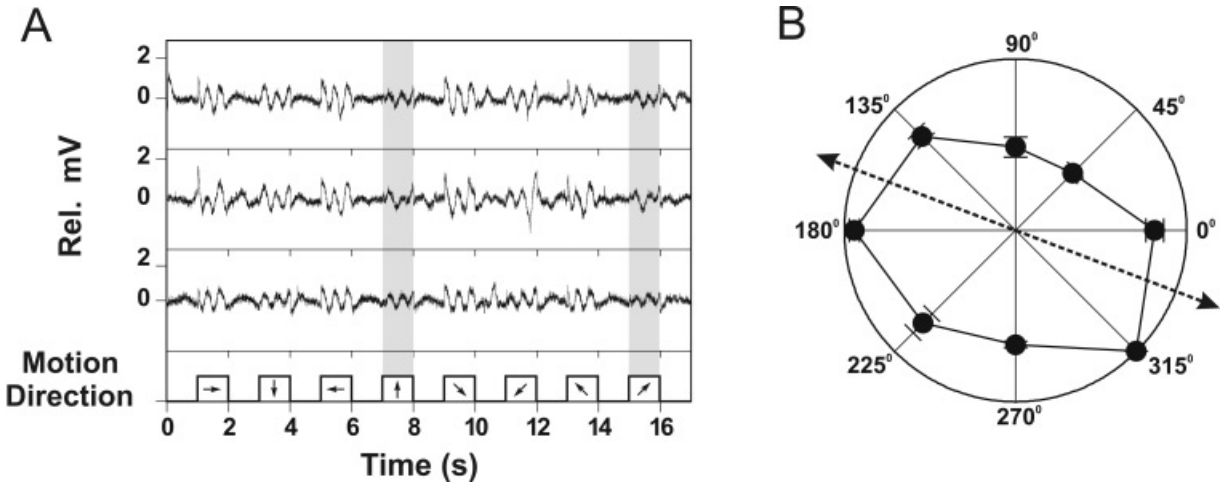

Fig. 6. Orientation- and weakly direction-selective responses of lamina amacrine iii to grating motion. (A) three successive presentations of wide-field grating motion in a sequence of eight directions. The raw data were high-pass fast Fourier-filtered to remove slow fluctuations below 1 Hz, then zeroed to a common baseline. Shaded bars indicate the two directions that produced the weakest responses. (B) Polar plot derived from the traces in A, showing normalized mean responses ($N = 3$, mean ± S.E.) as a function of motion direction. Each motion direction was presented for 1.0 s, preceded and followed by 1.0 s of a blank screen having the same mean luminance as the gratings. Response amplitudes were defined as the integrated rectified voltage (a sum of both positive and negative departures from the baseline) for 1100 ms from the start of each motion interval. The extra 100 ms allowed for recovery of the membrane voltage to baseline after cessation of motion. The preferred axis of orientation is at 159 deg (arrowed dotted line).

Though the intracellularly stained profiles in Fig. 2 clearly belong to lamina amacrines, it is unknown why it has not yet been possible to visualize an entire stained amacrine. Lamina amacrines have also been known to stain incompletely with silver techniques (Shaw, 1981; N.J. Strausfeld, personal observation). When a lamina amacrine neuron has been injected with dye, it is possible that in the very thin processes that connect different portions of the cell, the dye concentrations are too low to be distinguished from background fluorescence. An unusual feature of the dipteran brain is that illumination with violet to blue wavelengths produces strong background autofluorescence that obscures Lucifer yellow stained material (Fig 2, panel i). This problem is exacerbated in the peripheral optic lobe by the diffusion of ommochrome ocular accessory pigments into neighboring tissues during fixation, and is somewhat alleviated by removing the retina during dissection. As an alternative to Lucifer yellow, we have had good success at injecting lamina cells with neurobiotin and subsequently visualizing them with avidin-Texas Red (Fig. 2, panels ii–iv). Although our current procedure results in nonspecific fluorescence of glial cells and their cell bodies, as well as fainter staining of a subset of visual interneurons, the neurobiotin-injected material fluoresces particularly brightly, and can be clearly distinguished from the background when viewed with the naked eye.

Maximal peak-to-peak responses from amacrines and R1–R6 photoreceptors (from *ca.* 4–8 mV) were observed in response to full-field flicker or single bar motion at irradiances of approximately 4×10^{10} $q \cdot cm^{-2} \cdot s^{-1}$ (see Materials and methods). Previous investigators have reported obtaining similar response amplitudes from R1–R6 receptors at dimmer flash intensities (4–7 mV responses at 1 to 2×10^{9} $q \cdot cm^{-2} \cdot s^{-1}$; Scholes & Reichardt, 1969; Laughlin & Hardie, 1978). The discrepancy between these irradiance values appears to be due to differences in stimulus conditions. Whereas these previous studies employed fully dark-adapted flies and stimulus wavelengths that were very close to the 490 nm λ_{max} of R1–R6 receptors (Hardie, 1979), the flies in the present investigation were partly light adapted, and the spectral distribution of our CRT stimulus lies predominately above the λ_{max} of R1–R6 receptors. As lamina amacrines receive their inputs exclusively from R1–R6 receptors, they are expected to share the same spectral sensitivity. Thus, though the present results represent only one stimulus intensity, they suggest that unlike LMCs (Laughlin & Hardie, 1978), the absolute sensitivity of lamina amacrines is similar to that of R1–R6 receptors.

Since the basic visual response properies of lamina amacrines and photoreceptors are so similar, it is possible that some previously published recordings that were thought to have come from photoreceptors may actually represent lamina amacrines. At present, however, this seems unlikely for both methodological and anatomical reasons. In experiments that target insect photoreceptors, the typical procedure (cf. Hardie, 1979; Anderson & Laughlin, 2000) has been to aim the pipette tip toward a preselected retinal region *via* a small cut at the surface of the compound eye. With this technique, one expects to impale those portions of photoreceptors that reside entirely within the retina (namely, cell bodies or cytoplasmic regions adjacent to the rhabdomeres), and the pipette tip may never reach the lamina. On the other hand, if the pipette tip does reach the lamina, or if the lamina is specifically targeted (e.g. Scholes, 1969; Zettler & Weiler, 1976), it still seems much more likely that a large R1-R6 photoreceptor terminal would be impaled than a thin amacrine process.

Sign-conserving and sign-inverting responses of lamina neurons

Other than receptors, all of the eight types of lamina neurons that have previously been identified by intracellular recordings and dye fills exhibit sign-inverting responses. The large monopolar cells (LMCs) L1–L3 (Järvilehto & Zettler, 1973; Gilbert et al., 1991; Anderson & Laughlin, 2000), the small monopolar cells (SMCs),

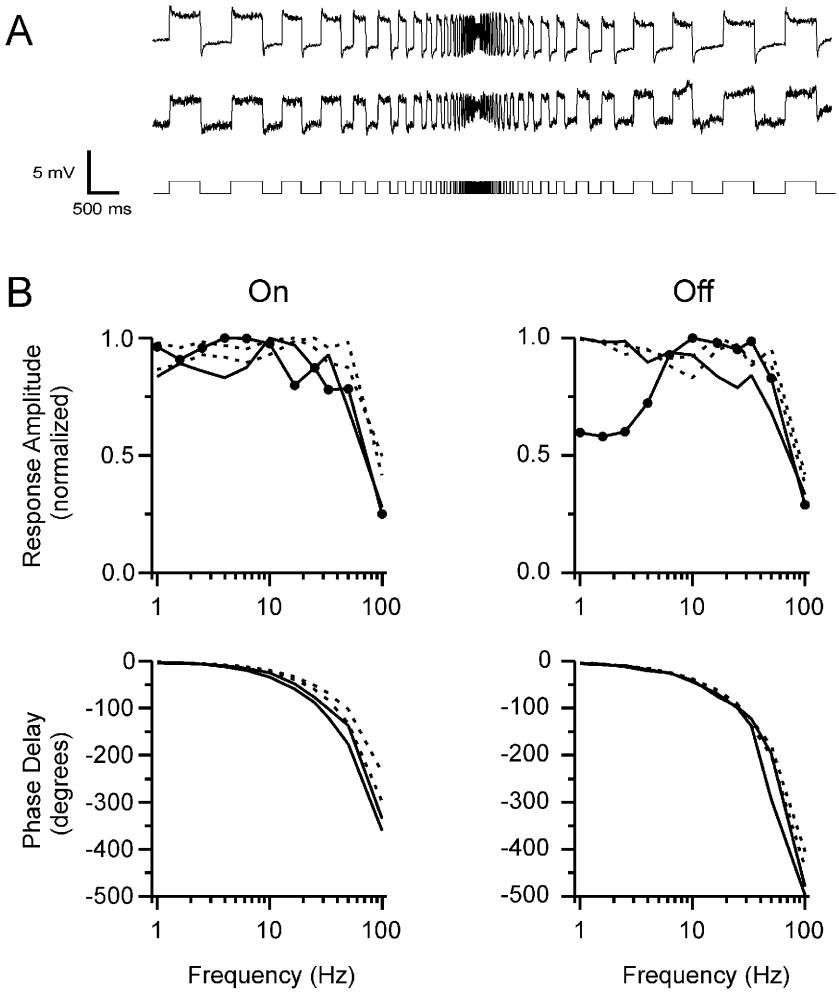

Fig. 7. Responses of lamina amacrines and photoreceptors as a function of contrast frequency. (A) Raw response of a photoreceptor (upper trace) and amacrine i (middle trace) to the full-field flicker ramp stimulus (bottom trace). (B) On- and Off-response amplitudes (upper plots) and phase delays (lower plots) of two lamina amacrines (solid lines) and photoreceptors (dashed lines), measured from responses such as those shown in A. The amplitudes in B are normalized to individual response maxima.

L4 and L5 (Douglass & Strausfeld, 1995), the "basket" T1 efferent neuron (Järvilehto & Zettler, 1973; Douglass & Strausfeld, 1995), the centrifugal neuron C2, and the type 1 lamina tangential cell (Lam Tan1; Strausfeld, 1970; Douglass & Strausfeld, 1995) all exhibit hyperpolarizing "On" responses and depolarizing "Off" responses. In contrast, the present results show that type 1 lamina amacrine cells have sign-conserving responses which are very much like those of photoreceptors.

Among all anatomically identified cell types that have processes within the lamina, only three have yet to be identified following an intracellular recording: the type 2 lamina tangential cell (Lam Tan2), the centrifugal neuron C3, and the type 2 lamina amacrine (Am2). Could any of the recordings we have attributed to type 1 lamina amacrines (Am1) have arisen from Lam Tan 2, C3, or Am 2 neurons? This is unlikely, because it would be difficult to mistake even partial stainings of these neurons with an Am1 cell. Lam Tan 2 processes, like those of Am 2 (Strausfeld & Nässel, 1980), reside only at the outer surface of the plexiform layer and should be easily distinguished from staining of the α processes of type 1 amacrines. Moreover, C3 and Lam Tan 2 have their principal dendritic fields in the inner and outer medulla, respectively, where they are likely to receive inputs from higher-order retinotopic neurons and thus should have significantly longer response latencies than we have seen here.

Implications of sign-conserving responses of lamina amacrine neurons

The demonstration that lamina amacrines have sign-conserving responses has interesting implications for the nature of neurotransmission from photoreceptors to amacrines. It is well established that histamine is the neurotransmitter used by the photoreceptors of various insects and other arthropods at synapses to LMCs (Nässel et al., 1988; Nässel, 1999; Stuart, 1999), and that the inhibitory postsynaptic responses of LMCs to histamine are directly gated by chloride channels (Hardie, 1989; Geng et al., 2002). In contrast, our data imply that neurotransmission from photoreceptors to lamina amacrines is excitatory. This suggests three basic hypotheses regarding the nature of photoreceptor-amacrine synapses: they could function *via* a metabotropic histamine receptor related to those of vertebrates, they could be electrical, or they could use an additional, nonhistamine neurotransmitter such as acetylcholine. The evidence for metabotropic histamine receptors in insects is controversial, with one molecular study suggesting there is no arthropod homologue to vertebrate metabotropic histamine receptors (Roeder, 2003). Although these observations do not exclude the possibility that such receptors may have evolved independently in vertebrates and invertebrates (Roeder, 2003), the rapid flicker responses of lamina amacrines are incon-

sistent with the slow temporal dynamics of conventional metabotropic receptors. This leaves the possibility of electrical synapses or a second type of transmitter. But whereas anatomical studies have described only chemical synapses between receptors and amacrines (Boschek, 1971; Strausfeld & Campos-Ortega, 1977), three studies provide evidence for the presence of acetylcholine in insect photoreceptors. In honey bee, histochemical tests have demonstrated acetylcholinesterase in the photoreceptors (Kral & Schneider, 1981). This enzyme has also been identified in developing photoreceptors of mid-pupal *Drosophila* (Wolfgang & Forte, 1989). Although the presence of the enzyme could underlie biochemical pathways unrelated to synaptic transmission, it is consistent with the possibility that fly photoreceptors employ a dual fast transmitter system. A more recent finding, that rhabdomeric photoreceptors of the *Drosophila* imago eyelet stain both for histamine and with an antibody against *Drosophila* choline acetyltransferase (Yasuyama & Meinertzhagen, 1999), is of special interest in this regard. If this antibody has not clearly revealed the enzyme in other photoreceptors, this may only be a matter of its relative concentration.

As for neurons that receive inputs from lamina amacrines, their responses may be either sign reversing (e.g. T1, Järvilehto & Zettler, 1973; Douglass & Strausfeld, 1995) or sign conserving (other type 1 lamina amacrines). This suggests that amacrine outputs also may involve more than one neurotransmitter or transmitter pathway. Currently, evidence that lamina amacrines are glutamate immunoreactive (Sinakevitch & Strausfeld, 2004) suggests that glutamate alone could serve both excitatory and inhibitory roles, as has been suggested for the outputs from mammalian photoreceptors to On- and Off-bipolar cells (Bloomfield & Dacheux, 2001). The situation in flies is complicated, however, by the fact that T1 also receives some inputs from photoreceptors (Campos-Ortega & Strausfeld, 1973).

Functional properties and possible functional roles of lamina amacrine neurons

Until now, the observation that amacrine dendritic fields can extend across several VSUs, coupled with the presence of connections among neighboring amacrines, has led many workers (including ourselves) to expect their receptive fields to encompass more than a single VSU. In a notable exception to this point of view, Shaw (1981) debated whether lamina amacrines might exhibit some degree of signal decrement that could result in functional isolation of individual α processes. Here, we have shown that amacrine responses to grating motion, stationary spots, and bar motion are all similar to those of photoreceptors. Given the larger dendritic fields of amacrines, these results suggest that lamina amacrines have fairly short space constants, meaning that passive conduction of local voltage fluctuations may decrement quite rapidly and not be strongly propagated to neighboring cartridges. This contrasts with vertebrate horizontal cells, which occupy an analogous position with respect to photoreceptor inputs but have receptive fields which are considerably wider than their dendritic fields (e.g. Tomita, 1965; Naka & Rushton, 1967; Lamb, 1976; Quian & Ripps, 1992). Nevertheless, the receptive-field information provided by the current results is constrained by the relatively low stimulus intensities provided by a CRT display. In future experiments, we plan to employ much brighter point-source stimuli which are more comparable to natural irradiances and may reveal more extensive spatial receptive fields.

If lamina amacrines mainly transmit activity that is localized to approximately one VSU, what are the implications for their possible roles in visual computations? The amacrine α processes receive inputs from photoreceptor R1–R6 terminals, and at each optic cartridge the α processes are presynaptic to the "basket" T1 efferent neuron. One T1 cell and an LMC (L2) from each optic cartridge converge at the dendrites of a small-field transmedullary cell, Tm1. Comparative anatomical studies (Buschbeck & Strausfeld, 1996) suggest that these neurons are elements of an evolutionarily conserved pathway leading to directionally selective motion-sensitive neurons, called bushy T5 cells (Douglass & Strausfeld, 1995). The small-field T5 cells, in turn, supply large motion-selective neurons of the lobula plate, a tectum-like neuropil that contributes to visual balance during flight. These relays from the lamina through the medulla to the lobula plate have been proposed to constitute the elementary circuit for directionally selective motion detection, with the lamina amacrines providing the first step in this pathway (Douglass & Strausfeld, 2003*a*; Higgins et al., 2004; Sinakevitch & Strausfeld, 2004). This ana-

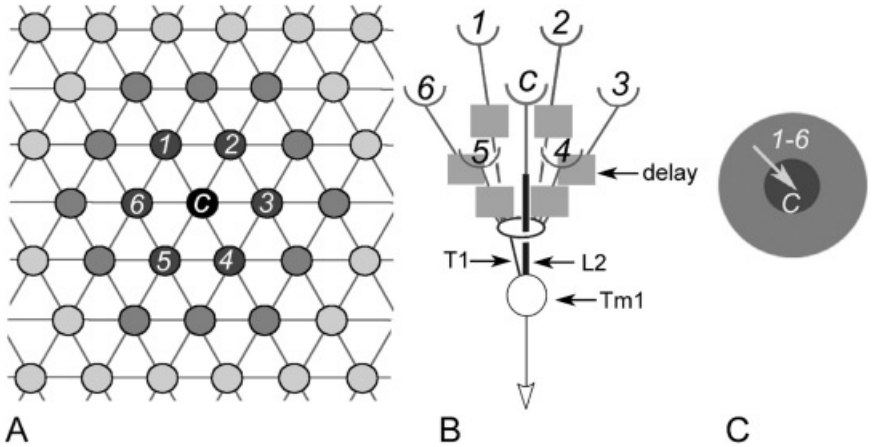

Fig. 8. Schematic views of the lamina amacrine network and its relationship with other lamina elements proposed to comprise the initial stage in motion detection. (A) Amacrine matrix, showing each optic cartridge linked by an isotropic network of distal amacrine tangential processes between surrounding cartridges. A T1 neuron at an optic cartridge (e.g. at "C") is proposed to receive amacrine inputs from the surrounding cartridges "1-6" and not from cartridge C. (B) Amacrine connections may provide information about local changes in receptor activity to a T1 neuron from receptors of surrounding cartridges, and thus VSUs "1-6". These connections involve 2–3 synaptic delays. Retinula cells of the central cartridge (VSU "C") synapse directly onto the L2 monopolar cell. (C) Convergence of T1 and L2 activity at Tm1 provides Tm1 with information about sequential changes in luminance occurring between any of the surrounding VSUs "1-6" and the central VSU "C".

tomically and physiologically inspired circuit involves multiple levels, thus departing from the traditional Reichard-Hassenstein model, which supposes that both the presence of motion and its direction are detected in a single step. The central hypothesis (Fig. 8) is that amacrine processes converging from the immediately surrounding optic cartridges drive the T1 pathway of a central optic cartridge, while the photoreceptors supplying this central cartridge drive its L2 monopolar cell. The present evidence for spatially localized activity in lamina amacrines appears to be consistent with the proposal that amacrine activity from neighboring optic cartridges converges to a central T1 cell. This does not exclude the possibility that inputs from amacrines to T1, L4, or L5 may also produce lateral inhibitory effects, for which there is some evidence in T1 based on evidence its receptive field is narrower than those of receptors (Järvilehto & Zettler, 1973).

In summary, the present recordings reveal several basic visual response properties of lamina amacrines which are relevant to their possible functional role(s). These properties include fast, photoreceptor-like responses to flicker, and spatial properties that are very localized and thus suggestive of passive conduction properties. Although our contrast frequency data were obtained by using a square-wave flicker stimulus, they agree qualitatively with previously published data from dipteran photoreceptors and LMCs involving either sinusoidally varied (Järvilehto & Zettler, 1973; Coombe et al., 1989) or pseudorandomly modulated (Juusola et al., 1994; Anderson & Laughlin, 2000) flicker stimulation. If lamina amacrines were to play a neuromodulatory role related to long-term aspects of light and dark adaptation and/or circadian rhythms, they would not necessarily need fast temporal properties, and might be expected to have larger receptive fields. Although the properties demonstrated here are consistent with a variety of computational roles including lateral inhibition, light/dark adaptation, motion processing, or edge processing, the only direct physiological evidence so far comes from the demonstration of orientation-selective motion responses, suggesting the involvement of lamina amacrines in processing the orientations of moving edges.

Acknowledgments

We would like to thank Drs. Konrad E. Zinsmaier and Charles M. Higgins for discussions, and two anonymous reviewers for their suggestions. This research was supported by NIH R01-RR08868.

References

Anderson, J.C. & Laughlin, S.B. (2000). Photoreceptor performance and the co-ordination of achromatic and chromatic inputs to the fly visual system. *Vision Research* **40**, 13–31.

Bloomfield, S.A. & Dacheux, R.F. (2001). Rod vision: Pathways and processing in the mammalian retina. *Progress in Retinal and Eye Research* **20**, 351–384.

Boschek, C.B. (1971). On the fine structure of the peripheral retina and the lamina of the fly, *Musca domestica*. *Zeitschrift für Zellforschung und Mikroskopische Anatomie* **110**, 369–409.

Braitenberg, V. (1967). Patterns of projection in the visual system of the fly. I. Retina-lamina projections. *Experimental Brain Research* **3**, 271–298.

Burkhardt, D. & Autrum, H. (1960). Die Belichtungspotentiale einzelner Sehzellen von *Calliphora erythrocephala* Meig. *Zeitschrift für Naturforschung* **15b**, 612–616.

Burton, B.G., Tatler, B.W. & Laughlin, S.B. (2001). Variations in photoreceptor response dynamics across the fly retina. *Journal of Neurophysiology* **86**, 950–960.

Buschbeck, E.K. & Strausfeld, N.J. (1996). Visual motion-detection circuits in flies: Small-field retinotopic elements responding to motion are evolutionarily conserved across taxa. *Journal of Neuroscience* **16**, 4563–4578.

Campos-Ortega, J.A. & Strausfeld, N.J. (1973). Synaptic connections of intrinsic cells and basket arborizations in the external plexiform layer of the fly's eye. *Brain Research* **59**, 119–136.

Coombe, P., Srinivasan, M.V. & Guy, R.G. (1989). Are the large monopolar cells of the insect lamina on the optomotor pathway? *Journal of Comparative Physiology A* **166**, 23–35.

Douglass, J.K. & Strausfeld, N.J. (1995). Visual motion detection circuits in flies: Peripheral motion computation by identified small-field retinotopic neurons. *Journal of Neuroscience* **15**, 5596–5611.

Douglass, J.K. & Strausfeld, N.J. (1996). Visual motion-detection circuits in flies: Parallel direction- and non-direction-sensitive pathways between the medulla and lobula plate. *Journal of Neuroscience* **16**, 4551–4562.

Douglass, J.K. & Strausfeld, N.J. (1998). Functionally and anatomically segregated visual pathways in the lobula complex of a calliphorid fly. *Journal of Comparative Neurology* **396**, 84–104.

Douglass, J.K. & Strausfeld, N.J. (2003*a*). Anatomical organization of retinotopic motion-sensitive pathways in the optic lobes of flies. *Microscopy Research and Technique* **62**, 132–150.

Douglass, J.K. & Strausfeld, N.J. (2003*b*). Retinotopic pathways providing motion-selective information to the lobula from peripheral elementary motion detecting circuits. *Journal of Comparative Neurology* **456**, 326–344.

Franceschini, N. (1975). Sampling of the visual environment by the compound eye of the fly: Fundamentals and applications. In *Photoreceptor Optics*, ed. Snyder, A.W. & Menzel, R., pp. 8–125. Berlin, Heidelberg, New York: Springer.

Geng, C., Leung, H.-T,, Skingsley, D.R., Iovchev, M.I., Yin, Z., Semenov, E.P,, Burg, M.G., Hardie, R.C. & Pak, W.L. (2002). The target of *Drosophila* photoreceptor synaptic transmission is a histamine-gated chloride channel encoded by *ort* (*hclA*). *Journal of Biological Chemistry* **277**, 42113–42120.

Gilbert, C., Penisten, D.K. & DeVoe, R.D. (1991). Discrimination of visual motion from flicker by identified neurons in the medulla of the fleshfly *Sarcophaga bullata*. *Journal of Comparative Physiology A* **168**, 653–673.

Hardie, R.C. (1979). Electrophysiological analysis of fly retina. I. Comparative properties of R1-R6 and R7 and 8. *Journal of Comparative Physiology A* **129**, 19–33.

Hardie, R.C. (1986). The photoreceptor array of the dipteran retina. *Trends in Neuroscience* **9**, 419–423.

Hardie, R.C. (1989). A histamine-activated chloride channel involved in neurotransmission at a photoreceptor synapse. *Nature* (London) **339**, 704–706.

Hengstenberg, R. (1982). Common visual response properties of giant vertical cells in the lobula plate of the blowfly *Calliphora*. *Journal of Comparative Physiology* **149**, 179–193.

Higgins, C.M., Douglass, J.K. & Strausfeld, N.J. (2004). The computational basis of an identified neuronal circuit for elementary motion detection in dipterous insects. *Visual Neuroscience* **21**, 567–586.

Ioannides, A.C. (1972) *Light adaptation and signal transmission in the compound eye of the giant water bug Lethocerus (Belastomatidae: Hemiptera)*. Ph.D. Thesis, Canberra National University, Australia.

Järvilehto, M. & Zettler, F. (1973). Electrophysiological-histological studies on some functional properties of visual cells and second-order neurons of an insect retina. *Zeitschrift für Zellforschung und Mikroskopische Anatomie* **136**, 291–306.

Juusola, M., Kouvalainen, E., Järvilehto, M. & Weckström, M. (1994). Contrast gain, signal-to-noise ratio, and linearity in light-adapted blowfly photoreceptors. *Journal of General Physiology* **104**, 593–621.

Kral, K. & Schneider, L. (1981). Fine structural localisation of acetylcholinesterase activity in the compound eye of the honeybee (*Apis mellifica* L.). *Cell and Tissue Research* **221**, 351–359.

Lamb, T.D. (1976). Spatial properties of horizontal cell responses in the turtle retina. *Journal of Physiology* **263**, 239–255.

Laughlin, S.B. (1981). Neural principles in the peripheral visual systems of invertebrates. In *Handbook of Sensory Physiology, VII/6B*, ed. Autrum, H., pp. 133–280. Berlin: Springer.

Laughlin, S.B. & Hardie, R.C. (1978). Common strategies for light adaptation in the peripheral visual systems of fly and dragonfly. *Journal of Comparative Physiology* **128**, 319–340.

Meinertzhagen, I.A. & O'Neil, S.D. (1991). Synaptic organization of columnar elements in the lamina of the wild-type in *Drosophila melanogaster*. *Journal of Comparative Neurology* **305**(2), 232–263.

Naka, K.I. & Rushton, W.A.H. (1967). The generation and spread of s-potentials in fish (cyprinidae). *Journal of Physiology* **192**, 437–461.

Nässel, D.R. (1999). Histamine in the brain of insects: A review. *Microscopy Research and Technique* **44**, 121–136.

Nässel, D.R., Holmqvist, M.H., Hardie, R.C., Hakanson, R. & Sundler, F. (1988). Histamine-like immunoreactivity in photoreceptors of the compound eyes and ocelli of the flies *Calliphora erythrocephala* and *Musca domestica*. *Cell and Tissue Research* **253**, 639–646.

O'Shea, M. & Adams, M.E. (1981). Pentapeptide (proctolin) associated with an identified neuron. *Science* **21**, 567–569.

Quian, H. & Ripps, H. (1992). Receptive-field properties of rod-driven horizontal cells in the skate retina. *Journal of General Physiology* **100**, 457–478.

Roeder, T. (2003). Metabotropic histamine receptors—nothing for invertebrates? *European Journal of Pharmacology* **466**, 85–90.

Scholes, J. (1969). The electrical responses of the retinal receptors and the lamina in the visual system of the fly *Musca*. *Kybernetik* **6**, 149–162.

Scholes, J. & Reichardt, W. (1969). The quantal content of optomotor stimuli and the electrical responses of receptors in the compound eye of the fly *Musca*. *Kybernetik* **6**, 74–79.

Shaw, S.R. (1981). Anatomy and physiology of identified non-spiking cells in the photoreceptor-lamina complex of the compound eye of insects, especially Diptera. In *Neurones Without Impulses: Their Significance for Vertebrate and Invertebrate Nervous Systems*, eds. Roberts, A. & Bush, B.M.H., pp. 61–116. Cambridge: Cambridge University Press.

Shaw, S.R. (1984). Early visual processing in insects. *Journal of Experimental Biology* **112**, 225–251.

Sinakevitch, I. & Strausfeld, N.J. (2004). Chemical neuroanatomy of the fly's movement detection pathway. *Journal of Comparative Neurology* **468**, 6–23.

Smakman, J.G.J., van Hateren, J.H. & Stavenga, D.G. (1984). Angular sensitivity of blowfly photoreceptors: Intracellular measurements and wave-optical predictions. *Journal of Comparative Physiology A* **155**, 239–247.

Strausfeld, N.J. (1970). Golgi studies on insects. Part II. The optic lobes of Diptera. *Philosophical Transactions of the Royal Society B* (London) **258**, 135–223.

Strausfeld, N.J. (1976). Mosaic organizations, layers, and visual pathways in the insect brain. In *Neural Principles in Vision*, ed. Zettler, F. & Weiler, R., pp. 245–279. Berlin, Heidelberg, New York: Springer.

Strausfeld, N.J. (1989). Beneath the compound eye: Neuroanatomical analysis and physiological correlates in the study of insect vision. In *Facets of Vision*, ed. Stavenga, D.G. & Hardie, R.C., pp. 317–359. Heidelberg: Springer.

Strausfeld, N.J. & Campos-Ortega, J.A. (1977). Vision in insects: Pathways possibly underlying neural adaptation and lateral inhibition. *Science* **195**, 894–897.

Strausfeld, N.J. & Li, Y. (1999). Organization of olfactory and multimodal afferent neurons supplying the calyx and pedunculus of the cockroach mushroom bodies. *Journal of Comparative Neurology* **409**, 603–625.

Strausfeld, N.J. & Nässel, D.R. (1980). Neuroarchitecture of brain regions that subserve the compound eyes of Crustacea and Insects. In *Handbook of sensory physiology, VII/6B*, ed. Autrum, H., pp. 1–133. Heidelberg: Springer.

Stuart, A.E. (1999). From fruit flies to barnacles, histamine is the neurotransmitter of arthropod photoreceptors. *Neuron* **22**, 431–433.

Tomita, T. (1965). Electrophysiological study of the mechanisms subserving color coding in the fish retina. *Cold Spring Harbor Symposia on Quantitative Biology* **30**, 559–566.

Washizu, Y., Burkhardt, D. & Streck, P. (1964). Visual field of single retinula cells and interommatidial inclination in the compound eye of the blowfly *Calliphora erythrocephala*. *Zeitschrift für Vergleichende Physiologie* **48**, 413–428.

Wolfgang, W.J. & Forte, M.A. (1989). Expression of acetylcholinesterase during visual system development in *Drosophila*. *Developmental Biology* **131**, 321–330.

Yasuyama, K. & Meinertzhagen, I.A. (1999). Extraretinal photoreceptors at the compound eye's posterior margin in *Drosophila melanogaster*. *Journal of Comparative Neurology* **412**, 193–202.

Zettler, F. & Weiler, R. (1976). Neuronal processing in the first optic neuropile of the compound eye of the fly. In *Neural Principles in Vision*, ed. Zettler, F. & Weiler, R., pp. 227–237. New York: Springer.